

**INDUCING UNIQUE POLYMERIC MORPHOLOGY BASED ON  
MOLECULAR ASSEMBLY: MODEL CASES FROM THERMOPLASTIC  
ELASTOMER SEBS AND/OR SUPRAMOLECULAR BENZOXAZINE**

Wonchalerm Rungswang

A Dissertation Submitted in Partial Fulfilment of the Requirements  
for the Degree of Doctor of Philosophy  
The Petroleum and Petrochemical College, Chulalongkorn University  
in Academic Partnership with  
The University of Michigan, The University of Oklahoma,  
and Case Western Reserve University

2011

128374894

**Thesis Title:** Inducing Unique Polymeric Morphology based on Molecular Assembly: Model Cases from Thermoplastic Elastomer SEBS and/or Supramolecular Benzoxazine

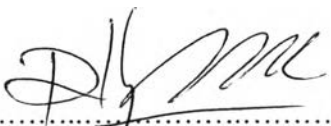
**By:** Wonchalerm Rungswang

**Program:** Polymer Science

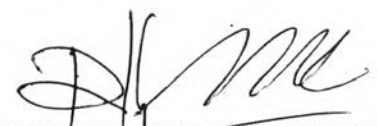
**Thesis Advisors:** Assoc. Prof. Suwabun Chirachanchai  
Assoc. Prof. Masaya Kotaki


---


Accepted by the Petroleum and Petrochemical College, Chulalongkorn University, in partial fulfilment of the requirements for the Degree of Doctor of Philosophy.

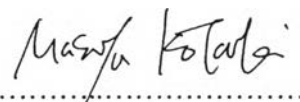
  
..... Dean  
(Asst. Prof. Pomthong Malakul)

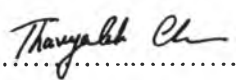
**Thesis Committee:**

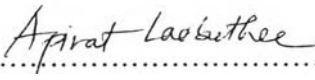
  
.....  
(Asst. Prof. Pomthong Malakul)

  
.....  
(Assoc. Prof. Suwabun Chirachanchai)

  
.....  
(Air Marshal Dr. Somsak Naviroj)

  
.....  
(Assoc. Prof. Masaya Kotaki)

  
.....  
(Dr. Thanyalak Chaisuwan)

  
.....  
(Asst. Prof. Apirat Laobuthee)

## ABSTRACT

4982005063: Polymer Science Program

Wonchalerm Rungswang: Inducing Unique Polymeric Morphology Based on Molecular Assembly: Model Cases from Thermoplastic Elastomer SEBS and/or Supramolecular Benzoxazine.

Thesis Advisors: Assoc. Prof. Suwabun Chirachanchai, Assoc. Prof. Masaya Kotaki, 114 pages

Keywords: Self-assembly/ Thermoplastic Elastomer/ Microdomains/ SEBS/ Electrospinning/ Thermosetting Nano-sphere/ *N,N*-Bis(2-hydroxyalkylbenzyl)alkylamine/ Polydiacetylene

The present work focuses on inducing the polymer morphology via the molecular self-assembly approaches. In the first part, an existence of ordered-structure microdomains, nano-phase separation, of thermoplastic elastomers in as-spun electrospinning fibers is clarified through a study case of SEBS triblock copolymer using two-dimensional small angle X-ray scattering (2D-SAXS) technique. The work also shows that when the molecular interaction is formed the microdomain direction can be controlled as seen in the case of benzoxazine monomer (BZ) to induce microdomain orientation to be parallel to the fiber axis based on the  $\pi$ - $\pi$  interaction between PS segment of SEBS and BZ monomer. In the second part, the work shows how the  $\pi$ - $\pi$  interaction between PS segment of SEBS and BZ monomer leads to molecular pocket-like structure to control the polymerization of BZ and give polyBZ nano-sphere which is a simple approach to prepare thermosetting nano-sphere. In the final part, the work covers supramolecular chemistry of BZ dimers, so-called *N,N*-Bis(2-hydroxyalkylbenzyl)alkylamine, to prepare a novel diacetylene (DA) monomer containing BZ dimers based cyclic ether which will be an effective pathway for solid-state polymerization to obtain polydiacetylenes.

## บทคัดย่อ

วันเฉลิม รุ่งสว่าง : การสร้างมอโฟโลยีของพอลิเมอร์ที่มีลักษณะเฉพาะโดยการจัดเรียงตัวเองในระดับโมเลกุล กรณีศึกษาจากเทอร์โมพลาสติกอีลาสโตเมอร์ เอสอีบีเอส และ(หรือ) เบนซอกซาซีนซูปปราโมเลกุล (Inducing Unique Polymeric Morphology Based on Molecular Assembly: Model Cases from Thermoplastic Elastomer SEBS and/or Supramolecular Benzoxazine) อ. ที่ปรึกษา: รองศาสตราจารย์ ดร. สุวณู จิรชาญชัย และ รองศาสตราจารย์ ดร.มาชายะ โคทาภิ, 114 หน้า

วิทยานิพนธ์ฉบับนี้มุ่งเน้นไปที่การสร้างมอโฟโลยีของพอลิเมอร์ที่มีลักษณะเฉพาะโดยการจัดเรียงตัวเองในระดับโมเลกุล ในส่วนแรก งานวิจัยนี้ได้พิสูจน์ให้เห็นที่ประจักษ์ถึงการมีอยู่ของโครงสร้างที่เป็นระเบียบของไมโครโดเมน การแยกเฟสในระดับนาโน ของเทอร์โมพลาสติกอีลาสโตเมอร์ในเส้นใย อีเล็กโตรสปินนิงผ่านกรณีศึกษาของ เอสอีบีเอส ไตรบล็อกโคพอลิเมอร์โดยใช้เทคนิคอิเล็กซเรย์มุมแคบสองมิติ งานนี้ยังแสดงให้เห็นถึงว่าหากมีแรงอันตรกิริยาระหว่างโมเลกุลแล้วเราสามารถควบคุมการจัดเรียงตัวของไมโครโดเมนได้ด้วยดังเห็นได้จากกรณีของเบนซอกซาซีนมอนอเมอร์ซึ่งสามารถเหนี่ยวนำการจัดเรียงตัวของไมโครโดเมนในทิศทางขนานกับแกนของเส้นใยได้ เนื่องจาก แรงอันตรกิริยาของ พันธะพาย-พาย ที่เกิดขึ้นระหว่างช่วงของพอลิสไตรีนในสายโซ่เอสอีบีเอส และเบนซอกซาซีนมอนอเมอร์ ในส่วนที่สอง งานวิจัยได้แสดงให้เห็นถึงแรงปฏิกิริยาของ พันธะพาย-พาย ระหว่างพอลิสไตรีนในสายโซ่เอสอีบีเอส และเบนซอกซาซีนมอนอเมอร์ นั้นนำไปสู่โครงสร้างคล้ายกระเปาะในระดับ โมเลกุลเพื่อที่จะควบคุมปฏิกิริยาพอลิเมอร์ไรเซชันของเบนซอกซาซีนมอนอเมอร์ให้ได้พอลิเบนซอกซาซีนที่มีลักษณะทรงกลมที่มีขนาดระดับนาโน ซึ่งเป็นวิธีการที่ง่ายในการเตรียมเทอร์โมเซตที่มีลักษณะทรงกลมที่มีขนาดระดับนาโนได้อย่างไร ในส่วนสุดท้าย งานวิจัยนี้ยังครอบคลุมถึง เคมี ซูปปราโมเลกุลของเบนซอกซาซีนไดเมอร์ หรือที่เรียกว่าสารประกอบ เอ็น,เอ็น-บิส(5-เมทิล-2-ไฮดรอกซีเบนซิล)เมทิลเอมีน เพื่อที่จะเตรียม ไดอะเซทิลีน มอนอเมอร์ซึ่งมีสารประกอบวงแหวนอีเธอร์ซึ่งเป็นวิธีที่มีประสิทธิภาพสำหรับปฏิกิริยาพอลิเมอร์ไรเซชันในสภาวะของแข็งเพื่อที่จะได้ พอลิไดอะเซทิลีนในขั้นต่อไป

## ACKNOWLEDGEMENTS

The present dissertation would not have been accomplished without his Thai supervisor, Professor Suwabun Chirachanchai, who not only provided his continuous guidance and inspiration, but also gave him the opportunities to experience doing the research in Japan and USA. Apart from academic guidance, he also acknowledged the lessons related to the personality development, originality, and life philosophy.

He would like to express his appreciation to his Japanese co-advisor, Associate Professor Masaya Kotaki, for the suggestions, worth advices, strong support, helpful comments and warm hospitality including all members in Kotaki research group during his stay in Japan.

He would like to express his appreciation to Professor Shinichi Sakurai for his guidance, valuable discussion and continuous support for small angle X-ray scattering (SAXS) measurements and interpretations. Also a sincere thank is expressed to Takuma Shimojima and Go kimura for their SAXS data processing and analyses.

He would like to express his appreciation to Professor Hatsuo Ishida and Associate Professor Tarek Agag for valuable comment and advices. He would like to extend his sincere thanks to all members in Ishida research group for their helps and good memories throughout his stay in Cleveland, USA.

A deep gratitude is expressed to Kiyoo Kato and Asahi Kasei Chemical Corporation, Japan, for kindly providing SEBS samples.

He would like to express his appreciation to Dr. Eiko Nakazawa, Akiko Fujisawa and Hitachi High-technologies Corporation for providing TEM microtome training at Hitachi Demonstrating Lab, Ibaraki, Tokyo, including Keiji Takeuchi for his warm hospitality during his training.

A deep gratitude is expressed to Assistant Professor Apirat Laobuthee (Department of Material Engineering, Faculty of Engineering, Kasetsart University) for his fruitful discussion and invaluable guidance in organic syntheses.

He also would like to take this opportunity to express his appreciation to all Professors who have tendered invaluable knowledge at the Petroleum and Petrochemical College (during his Master-Philosophy of Doctoral program), and at

Department of Materials Science, Faculty of Science (during his Bachelor program), Chulalongkorn University.

He is particularly grateful to Associate Professor Apisit Songsasen (Department of Chemistry, Faculty of Science, Kasetsart University) who encouraged his passion in Chemistry, and gave him invaluable suggestion for his one-year advisee ship in Kasetsart University.

He wishes to thank all members in SWB research group for giving him helps and good memories during his study.

He appreciates the Ph.D. scholarship from the Royal Golden Jubilee Ph.D. Program (PHD/0058/2550)), the Thailand Research Fund through His acknowledgement also extends to the Japan Student Services Organization (JASSO) for the financial support for his short-term research in Japan.

He is grateful for the scholarship and funding of thesis work provided by the Petroleum and Petrochemical College, and by the National Center of Excellence for Petroleum, Petrochemical, and Advanced Materials, Thailand.

Finally, he wishes to express his gratitude to his family for their support and understanding, especially, his grandmothers who have not only raise him with their love, but also encourage and inspire him to follow his dream in being scientist with limitless.

## TABLE OF CONTENTS

	<b>PAGE</b>
Title Page	i
Abstract (in English)	iii
Abstract (in Thai)	iv
Acknowledgements	v
Table of Contents	vii
List of Schemes	x
List of Figures	xi
List of Table	xvii
<b>CHAPTER</b>	
<b>I INTRODUCTION</b>	<b>1</b>
<b>II LITERATURE REVIEW</b>	<b>5</b>
2.1 Polymer Morphology	5
2.2 Block Copolymer (Thermoplastic Elastomer)	6
2.3 Polystyrene-block-poly(ethylene-co-butylene)-block-polystyrene triblock copolymer (SEBS)	7
2.4 Microphase Separation in Block Copolymer	8
2.5 Electrospinning Technique for Nano-fiber Fabrication and Microphase Separation in Electrospun Fibers	12
2.6 Polybenzoxazine (polyBZ)	14
2.7 Molecular Self-Assembly	15
2.8 Development of Supramolecular Chemistry Based on BZ Dimers ( N,N-bis(2-hydroxybenzyl)alkylamine Derivatives (HBA))	17

<b>CHAPTER</b>	<b>PAGE</b>
2.9 Polydiacetylenes (PDAs)	18
2.10 Points of the Research	19
<b>III EXISTENCE OF MICRODOMAIN ORIENTATION IN THERMOPLASTIC ELASTOMER THROUGH A CASE STUDY OF SEBS ELECTROSPUN FIBERS</b>	<b>21</b>
3.1 Abstract	21
3.2 Introduction	22
3.3 Experimental	23
3.4 Results and discussion	25
3.5 Conclusions	42
3.6 Acknowledgement	44
3.7 References	44
<b>IV DIRECTING THERMOPLASTIC ELASTOMER MICRODOMAIN PARALLEL TO FIBER AXIS: A MODEL CASE OF SEBS WITH BENZOXAZINE UNDER <math>\pi</math>-<math>\pi</math> STACKING CONFORMATION</b>	<b>47</b>
4.1 Abstract	47
4.2 Introduction	48
4.3 Experimental	50
4.4 Results and discussion	52
4.5 Conclusions	74
4.6 Acknowledgements	74
4.7 References	75



<b>CHAPTER</b>	<b>PAGE</b>	
<b>V</b>	<b>FORMATION OF THERMOSETS VIA MOLECULAR POCKET IN THERMOPLASTIC CHAIN: A SIMPLE AND DIRECT WAY TO NANOSPHERICAL THERMOSETS</b>	<b>78</b>
	5.1 Abstract	78
	5.2 Introduction	79
	5.3 Experimental	80
	5.4 Results and discussion	81
	5.5 Conclusions	87
	5.6 Acknowledgements	88
	5.7 References	88
<b>VI</b>	<b>SYNTHESIS OF POLYDIACETYLENE CONTAINING AZA-CROWN-ETHER BASED ON N,N-BIS(ALKYL-2- HYDROXYL)ALKYLAMINE DERIVATIVES AS A PENDANT MOIETY</b>	<b>90</b>
	6.1 Abstract	90
	6.2 Introduction	91
	6.3 Experimental	92
	6.4 Results and discussion	96
	6.5 Conclusions	104
	6.6 Acknowledgement	104
	6.7 References	104
<b>VII</b>	<b>CONCLUSIONS</b>	<b>106</b>
	<b>REFERENCES</b>	<b>107</b>
	<b>CURRICULUM VITAE</b>	<b>110</b>

## LIST OF SCHEMES

SCHEMES	PAGE
<b>CHAPTER II</b>	
2.1 Possible addition reaction of PEB polymerization	8
2.2 Synthesis of di-phenol and mono-phenol based benzoxazine monomer	14
2.3 Chemical structure of di-phenol BZ monomer and its polyBZ	15
2.4 Diagram showing the development of HBA supramolecules by Suwabun group research	18
<b>CHAPTER IV</b>	
4.1 Synthesis of cyclohexylamine-based bisphenol BZ and its curing reaction to polyBZ	50
4.2 Suspected mechanism for vitrification of PS segments via $\pi$ - $\pi$ interaction between aromatic rings of BZ and PS in SEBS chains	54
<b>CHAPTER V</b>	
5.1 Suspected mechanism of nanospherical thermoset formation via molecular pocket of thermoplastic chains indicating the role of aromatic pendant group in PS and PS segments in SEBS chain for molecular assembly formation with BZ followed by the curing in nano-scaled or micro-scaled channel	87
<b>CHAPTER VI</b>	
6.1 Synthesis of <b>2,4DM-pa</b> and <b>HBA-pa</b>	93
6.2 Synthesis of dibenzo-monoaza-based <b>HBA-pa</b> derivatives	94

SCHEMES	PAGE
6.3 Synthesis of dibenzo-monoaza-crown diacetylene monomers	95

## LIST OF FIGURES

FIGURE	PAGE
<b>CHAPTER II</b>	
2.1 (a) polarizing optical micrograph of spherulite of polyoxymethylene, (b) atomic force microscope (AFM) micrograph of crystalline-lamellar morphology of poly(ethylene terephthalate) (Reiter et al. 2002), and (c) scanning electron microscope (SEM) micrograph of shish kebab morphology of polyethylene (Somani et al. 2005).	6
2.2 Schematic of block copolymers represent in blue and red lines in various architectures: (a) linear AB di-block copolymer, (b) linear ABA tri-block copolymer, (c) Mixed-arm-star block copolymer, and (d) $(AB)_n$ star block copolymer.	7
2.3 Hierarchy structure of microdomains composing of polybutadiene (PB) as majority and a minority of polystyrene (PS) (Honeker and Thomas 1996).	9
2.4 Microdomain morphologies: (column A) BCC sphere, (column B) cylindere, (column C) gyroid and (column D) lamella with their (row a) 2D-SAXS patterns, (row b) SAXS profiles, and (row d) TEM micrographs (Heck et al. 1997) and (Mogi et al. 1992).	10
2.5 Phase diagram of symmetrical di-block copolymer melt simulated from full mean-field theory (Matsen and Bates 1996).	11
2.6 Shape evolution of poly(ethylene oxide) solution in the electrospinning process which time zero is when the first eruption appears (Reneker and Yarin 2008).	12

<b>FIGURE</b>	<b>PAGE</b>
2.7 TEM micrographs of: as-spun (A) SBS and (B) polystyrene- b- polyisoprene diblock copolymer (SI) fiber (Kalra et al. 2006); and annealed (C) SIS and (D) SI fiber (Ma et al. 2006).	13
2.8 Typical examples of supramolecular structure via: (A) hydrogen bonding (B) van der Waals forces, (C) $\pi$ - $\pi$ interactions and (D) metal coordination.	16
2.9 Typical preorganization of DA monomer for topochemical polymerization (Lauher et al. 2008).	19
<b>CHAPTER III</b>	
3.1 SEM micrographs of SEBS electrospun microfibers obtained from an accelerating voltage of 20 kV: (a) and (b) under 30 % RH; (c) and (d) under 23 % RH.	25
3.2 Cross-sectional TEM micrograph of SEBS electrospun fibers collected at a 1240 m/min take-up velocity at: (a) 25000 times and (b) 40000 times for magnification. PS microdomains stained with ruthenium tetroxide were appearing dark.	27
3.3 TEM micrographs of SEBS electrospun fibers collected at (a ) 31.5 m/min, and (b) 1240 m/min; and 2D-SAXS patterns of SEBS electrospun fibers collected at 31.5 m/min for: (c) in an air chamber, and (d) in ethanol-filled chamber; and (e) illustration of ethanol-filled chamber.	28

FIGURE	PAGE
3.4 (a) 2D-SAXS patterns in a logarithmic scale for the scattering intensity (b) schematic 2D-SAXS patterns, and (c) possible schematic models to represent (a) for SEBS film (A), and SEBS electrospun fibers collected at 31.5 m/min (B).	29
3.5 2D-SAXS patterns of the fibers collected at: (a) 31.5 m/min, (b) 310 m/min, (c) 620 m/min, (d) 1 240 m/min; and (e) intensity distribution as a function of the azimuthal angle $\phi$ along the elliptic peak (azimuthal scan) of the SEBS electrospun fibers collected at 31.5 m/min ( $\bullet$ ), 310 m/min ( $\circ$ ), 620 m/min ( $\blacktriangle$ ) and 1240 m/min ( $\triangle$ ).	33
3.6 2D-SAXS patterns of the fibers collected at (a) 620 m/min, (b) schematic draw including structural parameter, and (c) possible lamellar-microdomain models including structural parameter.	36
3.7 Parameters $q_m$ (the magnitude of $q$ vector at the peak), and $d$ (lamellar repeating periods) of the SEBS fibers collected at various take-up velocities.	38
3.8 Peak width $\sigma$ , and $\delta$ of the SEBS fibers collected at various take-up velocities.	38
3.9 Angle $\mu$ , and $\phi$ of the SEBS fibers collected at various take-up velocities.	39
3.10 Possible models of: (a) distorted-lamellar microdomains, (b) fragmented-lamellar microdomains in the SEBS fibers at various take-up velocities, (c) schematic grain size ( $\delta^{-1}$ and $\sigma^{-1}$ ) regarding to take-up velocities.	40

<b>FIGURE</b>	<b>PAGE</b>
3.11 2D-SAXS patterns in a logarithmic scale of: (a) 1240 m/min, and (b) 620 m/min and; (c) azimuthal-scan profile for annealed SEBS electrospun fibers collected at 1240 m/min (●) and 620 m/min (○).	42
<b>CHAPTER IV</b>	
4.1 2D-NMR NOESY contour plot of S50BZ50 in CDCl <sub>3</sub> at concentration of 3.9 x 10 <sup>-3</sup> % w/w.	52
4.2 DSC thermograms of : (a) SEBS film, (b) S85B35 film and (c) S75BZ25 film.	53
4.3 Fiber diameters of as-spun S75BZ25 electrospinning fibers at various take-up velocities including their SEM images; (a), (b), (c) and (d) for those fibers collected at 0 m/min, 310 m/min, 620 m/min, and 1240 m/min, respectively.	55
4.4 Circular average SAXS profiles of (a) SEBS film and (b) S75BZ25 film including their 2D-SAXS patterns of (c) SEBS film and (d) S75BZ25 film.	56
4.5 2D-SAXS patterns of (a) as-spun SEBS electrospinning fibers collected at 310 m/min, and as-spun S75BZ25 electrospinning fibers collected at : (d) 31.5 m/min, (g) 310 m/min, (j) 620 m/min and (m) 1240 m/min, (b), (e), (h) and (k) are schematic illustrations highlighting the features of the 2D-SAXS patterns of (a), (d), (g) and (j), respectively, (f), (c) and (i); and (i) are possible models to represent (I) distorted-lamellar, (II) oblique-herringbone and (III) parallel-herringbone structure, respectively.	59

FIGURE	PAGE
4.6 Structural parameters of as-spun electrospinning fibers collected at various take-up velocities: lamellar repeating periods of SEBS (●) and S75BZ25(○); peak width parameters $\sigma$ and $\delta$ of SEBS (▲) and (■), and S75BZ25 ( $\Delta$ ) and ( $\square$ ); angle parameters $\mu$ and $\phi$ of SEBS (◆) and (▼) and S75BZ25 (▽), (◇), respectively.	63
4.7 Persistence length of the fragmented lamellae ( $l_p$ ), packing angle ( $\alpha$ ) and number of the packed lamellae in the grain ( $m$ ), where arbitrary constant ( $k$ ) in equation (1), (2) and (4) was assumed to be unity, of SEBS (●), (▲) and (■); and S75BZ25 (○), ( $\Delta$ ) and ( $\square$ ) as-spun electrospinning fibers, respectively, collected at various take-up velocities.	65
4.8 Schematic illustrations showing the changes of lamellar microdomain orientation, representing in individual grain, of SEBS and S75BZ25 as-spun electrospinning fibers at various take-up velocities. Note that these are quantitatively based on structural parameters evaluated from 2D-SAXS patterns.	68
4.9 (A) 2D-SAXS patterns of the post-cured S75BZ25 electrospinning fibers collected at : (a) 31.5 m/min, (b) 310 m/min, (c) 620 m/min and (d) 1240 m/min, and (B) SAXS profiles of : (a) as-cast SEBS film, (b) pre-cured S75BZ25 film, (c) post-cured S75BZ25 film and post-cured S75BZ25 electrospinning fibers collected at : (d) 31.5 m/min, (e) 310 m/min, (f) 620 m/min and (g) 1240 m/min. The fibers were fixed in adhesive epoxy before curing at 170°C for 3 hours.	71



<b>FIGURE</b>	<b>PAGE</b>
<p>4.10 Relative intensity distribution as a function of the azimuthal angle <math>\varphi</math> along the first-order peak (azimuthal scan) (a) in the 2D-SAXS pattern of post-cured S75BZ25 electrospinning fibers collected at: (●) 31.5 m/min, (○) 310 m/min, (▲) 620 m/min and (Δ) 1240 m/min, and Herman's orientation functions (<math>f</math>) for the peaks of the azimuthal scan at <math>\varphi = 90^\circ</math> (●) and at <math>\varphi = 0^\circ</math> (○) of post-cured S75BZ25 electrospinning fibers collected at various take-up velocities.</p>	73

## CHAPTER V

<p>5.1 FT-IR spectra of : (a) cured neat-BZ resin, (b) cured S50BZ50 film, and (c) nanospheres extracted from S50BZ50 by toluene</p>	82
<p>5.2 TEM micrographs (above images) and size distribution (below graphs) averaged from 200 spheres of BZ nanosphere for: (a) and (f) S10BZ90; (b) and (g) S25BZ75; (c) and (h) S50BZ50; (d) and (i) S75BZ25; and (e) and (j) S90BZ10.</p>	83
<p>5.3 SEM images of the cured-film mixtures ((a)-(e)) and TEM images of the extracted BZ-thermosets ((f)-(j)) of: (a) and (f) PS25BS75; (b) and (g) S25BZ75; (c) and (h) PBAT25BZ75; (d) and (i) PC25BZ75; and (e) and (j) CPE25BZ75 prepared by slow (□) and fast heating (■) at 60°C.</p>	84
<p>5.4 2D-NMR NOESY contour plot of a <math>3.9 \times 10^{-3}</math> %w/w of S50BZ50 in <math>\text{CDCl}_3</math>.</p>	85

FIGURE	PAGE
5.5 $^1\text{H}$ -NMR $T_1$ relaxation of BZ monomer of each proton in a $3.9 \times 10^{-3}$ %w/w $\text{CDCl}_3$ for: (a) S50BZ50, (b) PBAT50BZ50, (c) PC50BZ50 and (d) CPE50BZ50. $^1\text{H}$ of BZ monomer represents (●) H1 $\delta$ 6.97 ppm, (▲) H2 $\delta$ 6.82 ppm, (■) H3 $\delta$ 6.68 ppm, (◆) H4 $\delta$ 4.97 ppm, (○) H5 $\delta$ 4.06 ppm, ( $\Delta$ ) H6 $\delta$ 2.78 ppm, (□) H7 $\delta$ 1.99 ppm, ( $\diamond$ ) H8 $\delta$ 1.78 ppm and ( $\heartsuit$ ) H9 $\delta$ 1.29 ppm.	86

#### CHAPTER VI

6.1	FT-IR spectra of (a) <b>2,4DM-pa</b> , and (b) <b>HBA-pa</b> .	97
6.2	$^{13}\text{C}$ NMR (A) and ESI-mass (B) spectra of <b>HBA-pa</b> .	98
6.3	FT-IR spectra of (a) <b>HBA-pa</b> , (b) <b>1</b> and, (c) <b>13c2-pa</b> .	99
6.4	ESI-mass spectra of <b>13c2-pa</b> and <b>14c3-pa</b> .	101
6.5	$^1\text{H}$ NMR spectra of (a) <b>HBA-pa</b> , compound (b) <b>1</b> and (c) <b>13c2-pa</b> .	101
6.6	$^1\text{H}$ (A) and $^{13}\text{C}$ (B) NMR spectra of (a) <b>14c3-pa</b> , and (b) <b>14c3-DA</b> .	103

**LIST OF TABLES**

<b>TABLE</b>		<b>PAGE</b>
<b>CHAPTER III</b>		
3.1	Peak positions, $q_0$ and $q_{90}$ , and lamellar repeating period for $\varphi = 0^\circ$ and $\varphi = 90^\circ$ , respectively, obtained from 2D-SAXS patterns of SEBS electrospun collected at various take-up velocities compared with those of bulk film	34